Studii şi Cercetări Ştiinţifice 2023, **24** (2), pp. 155 – 171
Chimie şi Inginerie Chimică, Biotehnologii, Industrie Alimentară

Scientific Study & Research
Chemistry & Chemical Engineering, Biotechnology, Food Industry *ISSN 1582-540X*

ORIGINAL RESEARCH PAPER

ASSESSMENT OF MICROPLASTICS IN PERSONAL CARE PRODUCTS BY MICROSCOPIC METHODS AND VIBRATIONAL SPECTROSCOPY

Andreea Laura Banica[1,2*], Raluca Maria Bucur (Popa)[1*], Ioana Daniela Dulama[2], Ioan Alin Bucurica[2], Raluca Maria Stirbescu[2], Cristiana Radulescu[1,2,3]

[1]Politehnica University of Bucharest, Doctoral School Chemical Engineering and Biotechnology, 060042 Bucharest, Romania
[2]Valahia University of Targoviste, Institute of Multidisciplinary Research for Science and Technology, 130004 Targoviste, Romania
[3]Valahia University of Targoviste, Faculty of Sciences and Arts, 130004 Targoviste, Romania

*Corresponding author: banica.andreea@icstm.ro; ralucamaria.bucur@gmail.com

Received: May, 24, 2023
Accepted: June, 28, 2023

Abstract: Primary microplastics, known as microbeads (μBs), are found in personal care and cosmetic products (PCCPs) being used as an ingredient for physical abrasion on human body surface. Due to the fact that μBs has sizes less than 0.8 mm, sometimes even less than 0.1 mm, they can be ingested by many organisms, being transmitted in the food chain. The development of a method for isolating the microplastics from the matrix of branded PCCPs samples (i.e., shower gel, body spray) using ultrasound technique at constant temperature and pressure, high-performance vacuum filtration method with various high-purity filtration membranes (e.g., cellulose) was the first objective of this study. The second objective was to combine vibrational spectroscopy techniques (i.e., Fourier-transform infrared μ-spectroscopy) with optical microscopy, to investigate the morphology and chemical composition of MPs. Microplastics were identified in all five brands of analyzed products. Thus, an average value of 420 μBs/100 g in shower gel and 200 μBs/100 mL in body sprays was determined; the identified colors were black (mostly), blue, yellow, brown, green, and red. The observed sizes varied from tens of micrometers to a few centimeters in some cases and the thickness reached 10 μm. From visual (microscopy) and chemical (μ-FTIR spectroscopy) point of view the structure was mostly like polypropylene fibers, smaller and having glossy mate appearance.

Keywords: *body spray, fibers, PCCP, polymer, shower gel*

© 2023 ALMA MATER Publishing House, "VASILE ALECSANDRI" University of Bacău. All rights reserved.

INTRODUCTION

In the last decade, several studies have reported that microplastics (MPs) have been found in a variety of personal care and cosmetic products (PCCPs), including toothpastes, shampoos, cosmetics and shaving products, emulsion stabilizers and skin conditioning products [1 - 7]. MPs are found in matrices having different levels of complexity and due to this fact, the protocols of physicochemical analysis are greatly different. In this respect, MPs particles from PCCPs have different morphology such as fibers, pellets, fragments, and microbeads, from different types of polymers, at different sizes, sharps, color and forms [8]. The most common polymer types found in PCCPs composition are polyethylene (PE) but polyethylene terephthalate (PET), polypropylene (PP), polymethyl methacrylate (PMMA), nylons (PA), polyester (PES), and polyurethanes (PU) [2, 9, 10]. Primary microplastics, from PCCPs, called microbeads (μBs), are the ingredients able to offer abrasive properties on human body surfaces, such as teeth and skin [5]. During the times, μBs with sizes less than 0.8 mm and sometimes even less than 0.1 mm [11] and well-established durability, have replaced natural materials (inorganic powders, naturally introduced fruit peels and seeds) from various PCCPs [12]. Unfortunately, the μBs are easily found in the environment, can be ingested by various organisms, and finally are transferred in the food chain [13 - 16].
On the other hands, MPs contain of approximately 4 % chemical additives (e.g., phthalates, bisphenol A etc.) and have the capacity to adsorb several emerging toxic contaminants (e.g., PCBs, pesticides, PAHs, dioxins, perfluorinated alkyl compounds, synthetic musk, metals toxic, etc.) from the environment [15, 17, 18], amplifying the risk to humans' health, especially to children [19, 20].
Currently, the consumer demand for PCCPs is linked harmoniously by modern aesthetic practice and foretimes these products must be safety in terms of synthetic chemical compounds. In this regard, this study aims to provide a brief description of sampling, isolation, detection, and quantification of MPs from two categories of skin care products. In addition, preliminary investigations such as optical microscopy (OM) and micro-Fourier transform infrared spectroscopy (μ-FTIR) are performed in order to characterize the MPs matrix, in terms of morphology and chemical composition.

MATERIALS AND METHODS

Materials and reagents

In the present study where chosen products from the personal care and beauty category (shower gels and body spray – Table 1). The selection of cosmetic samples was based on (1) the use predominance, (2) the aspect of the product, (3) the purchase costs and (4) brand notoriety. Samples were coded and stored at room temperature until analysis.

Table 1. *Studied samples description*

Sample code	Product type	Active ingredients (declared by producer)
CtGD	personal care products (shower gels)	water, sodium laureth sulfate, acrylates copolymer, cellulose, perfume (fragrance), PEG–7 glyceryl cocoate, TEA-laurly sulfate, lauryl betaine, *Prunul armeniaca* (apricot) seed powder, *Pyrus malus* (apple) fruit extract, *Viola odorata* leaf extract, sorbitol, citric acid, phenoxyethanol, triethanolamine, sodium benzoate, α–isomethyl ionone, propylene glycol, CI 17200 (red 33, pigment), CI 61570 (green 5, pigment).
NaGD		water, sodium laureth sulfate, glycerin, coco-glucoside, sodium chloride (salt), cocamidopropyl betaine (from coconut oil), PEG-40 hydrogenated castor oil, perfume, *Aloe barbadensis* (aloe vera) extract, panthenol (provitamin B_5), betaine, citric acid, sodium benzoate, potassium sorbate, coumarin, CI 42090 (blue 1, pigment), CI 19140 (yellow 5, pigment), CI 42051 (blue 5, pigment).
NiGD		water, sodium laureth sulfate, cocamidopropyl betaine, acrylates copolymer, PEG–7 glyceryl cocoate, perfume, *Helianthus annuus* seed oil, glycerin, glyceryl glucoside, PEG–40 hydrogenated castor oil, sodium chloride, PEG–200 hydrogenated glyceryl palmate, benzophenone–4, lactose, microcrystalline cellulose, sodium lauryl sulfate, trisodium EDTA, phenoxyethanol, ethylparaben, methylparaben, geraniol, linalool, butylphenyl methylpropional, benzyl alcohol, limonene, CI 77492 (yellow 11, pigment), CI 42090 (blue 1, pigment).
IBS	beauty skin products (body sprays)	denatured alcohol, water, perfume, diethylhexyl, homosalate, butyl methoxybenzoylmethane, ethylhexyl, crosspolymer-6 polyacrylate, limonene, hydroxycitronellal, alpha-isomethyl ionone, coumarin, linalool, calcium titanium borosilicate, titanium dioxide, CI 14700 (red 4, pigment), CI 17200 (red 33, pigment).
BBS		denatured alcohol, water, fragrance, polyacryldimethylammonium, taurate, benzyl salicylate, linalool, limonene, citronellol, alpha-isomethyl ionone, coumarin, calcium borosilicate, tin oxide, silicon, CI 77891 (white 6 piment), CI 77491 (red iron oxide, pigment).

To avoid possible contamination with airborne microplastics, all the actions were carried out in the laboratory on surfaces previously cleaned with 70 % ethanol (according to the procedure described by Zhang *et al*. [21]). In the initial stage of the research, the used materials (Erlenmeyer beakers, graduated cylinders, pipettes, watch glass, Petri dishes, etc.) were sanitized in the first phase by washing with distilled water and washing acid (Nitric acid 2 %) and then sterilized at a temperature of 100 °C for 48 h in a forced convection oven, Venticell® type (BMT Medical Technology). The reagents used in the present study were of high purity: sodium dodecyl sulfate (≤ 98.5 %) (Merck) and hydrogen peroxide 30 – 31 % (Merck) and nitric acid 65% (Lachner). Liquid reagents were also filtered before use.

The samples were filtered using filter paper with a porosity of 12 - 15 µm, VWR® Grade 413 (VWR International). They were stored in Petri dishes previously sterilized in an oven. The ultrasonication of the samples was carried out in an ultrasonic bath type VWR® Ultrasonic Cleaner USC – TH (VWR International LLC.), and the filtration was carried out using a three-station filtration system and having a vacuum pump with a flow rate of 18 $L \cdot min^{-1}$.

Isolation/Extraction of microplastics

Chemical digestion is an optimal method for highlighting microplastics present in cosmetic products because it allows the destruction of the organic matrix in an efficient way. The present study used chemical treatments to obtain efficient and rapid methods for separating microplastics. Chemical digestion can be classified into two categories: alkaline and acid treatments; both treatments were effective in degrading the organic matrix without distorting the structure of the microplastics [22].
After performing the preliminary tests in order to obtain the most optimal extracting method of MPs from the analyzed samples, the recipe identified as the most favorable is presented in the following: in a vessel (Erlenmeyer beaker) - covered to avoid contamination with airborne MPs - 5 g shower gel sample or 10 mL body spray sample were mixed with 0.5 g or 1 g of sodium dodecyl sulfate (98.5 %) and 500 mL of distilled water. The samples thus obtained were stirred for 10 min at 200 rpm at room temperature and left to stabilize for 10 min. In the next phase it was performed the ultrasonication for 30 min at 40 – 45 °C, followed by vacuum filtration. The filters used for filtration process were dried in a desiccator for 48 h and stored in Petri dishes until physicochemical investigation.

Analytical techniques

Depending on the size of the samples and the need to highlight certain important details, the magnification factors used were 10X, 20X, 40X, and 100X, respectively. In this regard, the samples were examined using both transmitted and reflected light work modes using Primo Star (Carl Zeiss) and Stemi 2000c optical microscopes. These two microscopes were chosen due to the fact that they can be easily adapted to different types of samples, regardless of their nature. Image acquisition was performed using Zen proprietary software and Axiocam 105 digital video camera, both also manufactured by Carl Zeiss, Jena, Germany.
In FTIR microscopy and chemical imaging, HYPERION represents maximum sensitivity at the highest spatial resolution. It is specifically designed to provide the highest performance for visual examination and infrared analysis of any sample [23]. Before any material can be studied using FTIR microscopy, the region of interest must be identified. However, many microscopic samples lack contrast in the visible image. The microscope offers a variety of contrast enhancement strategies for visual inspection of samples in transmission and reflection.
The image of the sample is displayed not only on the computer's OPUS software, but also on an LCD screen built into the microscope. This second LCD panel allows sample placement and identification of the region of interest in the sample more easily. All visual images are recorded along with measured infrared spectra and sampling areas. Eyepieces are always accessible, providing a high-quality view of the sample. The region of interest can be detected even on samples with very low visual contrast [24 - 26].
Most microscopic samples should be between 5-15 µm in size for transmission µ-FTIR examination. Samples are measured in reflection if they are deposited on reflective substrates (KBr) [27]. However, many samples are neither transparent nor blocking the beam, so they can be easily studied using the attenuated total reflection (ATR) mode. As a result, the quality and utility of the ATR lens are critical for most applications [28, 29].

The spectral range can be extended from mid-infrared to near-infrared (NIR) and even visible (VIS, up to 25,000 cm^{-1}) and far-infrared (FIR, up to 80 cm^{-1}) [30]. The microscope is developed to achieve maximum sensitivity while maintaining maximum lateral resolution. In both transmission and reflection, apertures can be positioned in conjugate image planes separately before and after sampling [31, 32]. The spatial resolution of FTIR microscopic investigation is limited only by the diffraction of the input light [30].

The microscope's custom ATR objective (20X) ensures a good observation of the material without reducing the infrared light emission. The ATR crystal is positioned on the high-precision column mechanism to enable infrared acquisition once sample locations are established in the visual image. During data acquisition, the internal pressure sensor ensures repeatable sample-to-crystal contact [33, 34]. By combining automatic ATR mapping with the optional automatic z unit for the motorized x-y stage, even large sample regions can be studied with high spatial resolution. Different pressures at the ATR objective can be adjusted to suit soft to very hard samples. They are built from materials with a high refractive index (germanium or silicon), allowing them to investigate even dark materials. In addition, the ATR crystal functions as a solid immersion lens, increasing the spatial resolution achievable with ATR by a factor equal to the refractive index of the ATR crystal (germanium = 4) compared to transmission or reflection measurements [35 - 37].

OPUS software is an easy-to-use, powerful, all-in-one program that provides easy control over the microscope. It has the most extensive set of data capture, processing and evaluation features. The software user interface can be adapted for routine laboratory analysis as well as specialized research and development applications. To preserve data integrity and ease data processing, all resulting spectra, visual images, IR images, spectra are kept in a single file. Data collection with the μ-FTIR is straightforward as it is driven by the OPUS Software (OPUS 7.5). OPUS includes a number of algorithms for extracting useful information from simple or 3D measured data. The resulting infrared images can be displayed in various 2D and 3D viewpoints on top of or alongside the visible image [38].

Technical data of the HYPERION 2000 microscope: detector MCT D326 0 25 (SN J-19374), cooled with liquid nitrogen; motorized table with the size of 75 x 50 mm; 4X objective for visual observation; 15X transmission objective; 20X ATR objective; objective for self-calibration of all gratings and all laser lines.

RESULTS AND DISCUSSION

Through optical microscopy technique were identified MPs on the surface of the filters used in the filtration process. It served not only for identification purposes but also to characterize MPs according to shape and size. Thus, from the point of view of shape, MPs were identified in a remarkable number, having a cylindrical, rectangular, filiform/ thread-like or irregular appearance, etc. Some of the analyzed filters presented MPs of irregular shape, most likely obtained through actions of a mechanical nature, probably intentional (the main arguments being their nature and the target population for which the cosmetic product was intended).

In the case of CtGD sample were identified not less than 22 MPs in which case the highest number is represented by the black ones (18) followed by blue (2), red and yellow (1) (Table 2, Figure 1).

Table 2. *Identification by color of the MPs discovered on the surface of the analyzed filters (personal care products)*

Sample code	Color and number of MPs							Total number of MPs
	Black	Red	Blue	Yellow	Pink	Grey	Brown	
CtGD	18	1	2	1	nd*	nd*	nd*	22
NaGD	20	nd*	4	1	1	1	3	30
NiGD	4	nd*	6	nd*	nd*	nd*	1	11

nd = unidentified*

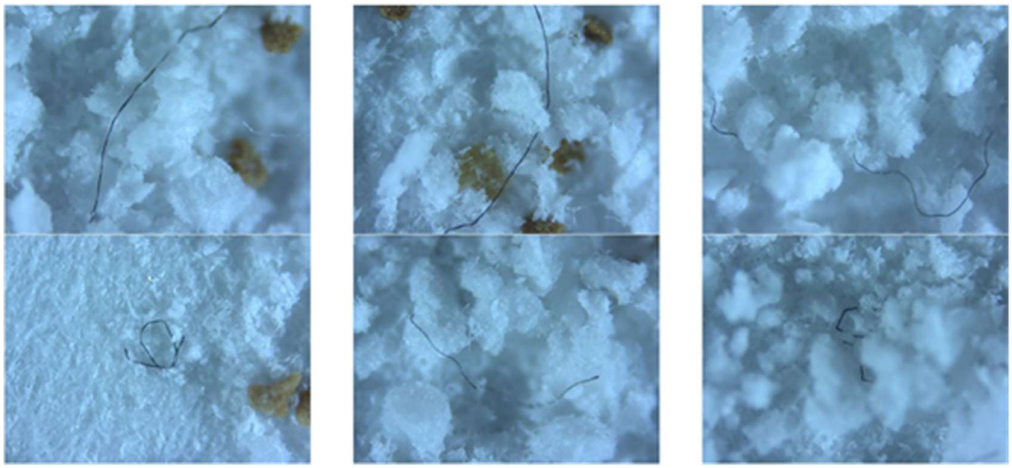

Figure 1. *Optical microscopy for CtGD sample (Primo Star 40X)*

On the other hand, in the case of NaGD the total number of MPs overpass the previous sample and recording a number of 30 MPs with an even higher number of black (20) and blue (4) but with the same quantity of yellow, pink, grey and brown (1) but with no red whatsoever (Table 2, Figures 2 and 3).

Figure 2. *Optical microscopy for NaGD sample (Primo Star 40X)*

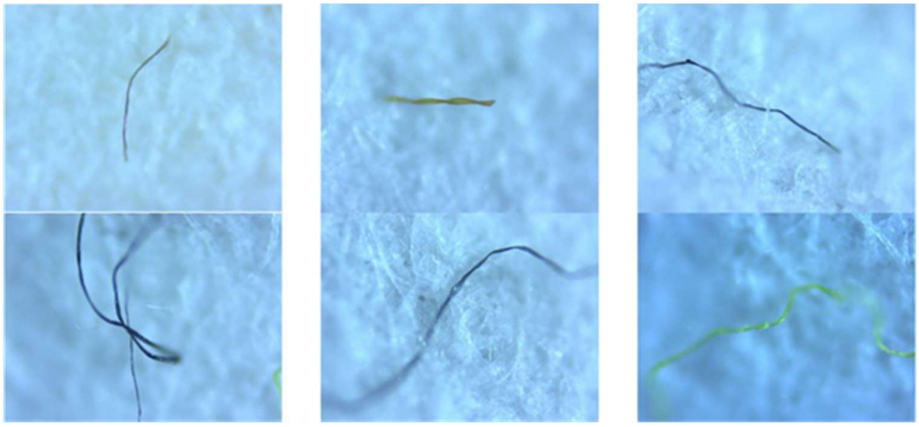

Figure 3. *Optical microscopy for NaGD sample (Primo Star 100X)*

For the last sample NiGD, shown in the Table 2 and Figures 4 and 5, it was highlighted a reasonable difference of MPs content, as the total number was with nineteen MPs less than NaGD and eleven than CtGD, furthermore, the color distribution shown that only four were black MPs but an increased number of blue ones (6) and just only one brown.

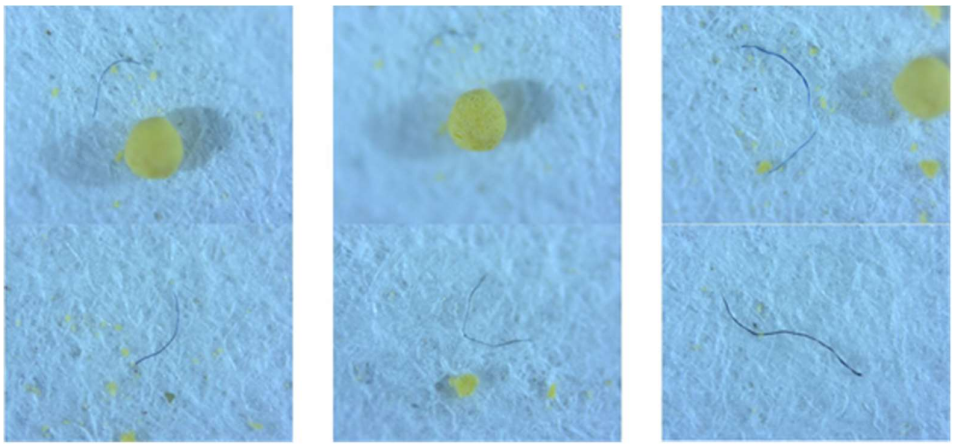

Figure 4. *Optical microscopy for NiGD sample (Primo Star 40X)*

Figure 5. *Optical microscopy for NiGD sample (Primo Star 100X)*

The total number of the MPs observed on the filtered sample from the personal care products and the overall distribution by color of the MPs are presented in Figures 6 and 7.

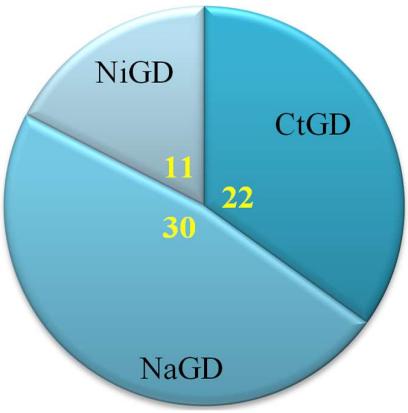

Figure 6. *Total number of the MPs discovered on filters surface (for the personal care products studied)*

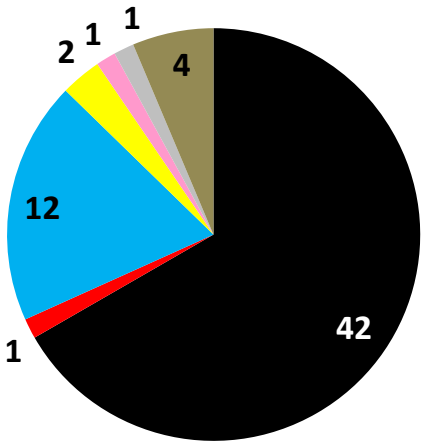

Figure 7. *Overall distribution by color of the MPs identified on filters surface (for the personal care products studied)*

In the case of IBS sample (Table 3, Figure 8) were identified 19 MPs for which the highest number is represented by the black ones (15) followed by red and brown (2).

Table 3. *Identification by color of the MPs discovered on the surface of the analyzed filters (beauty products samples)*

Sample code	Color and number of MPs					Total number of MPs
	Black	Red	Blue	Brown	Yellow	
IBS	15	2	nd*	2	nd*	19
BBS	14	2	2	2	1	21

nd = unidentified*

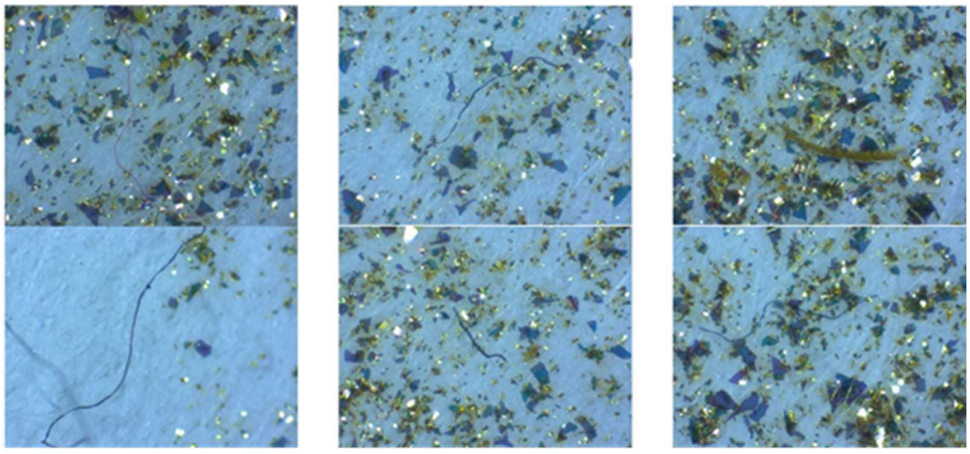

Figure 8. *Optical microscopy for IBS sample (Stemi-2000c 40X)*

On the other hand, in the case of BBS (Table 3, Figure 9), the total number of MPs overpasses just a bit the previous sample and records a total number of 21 MPs with an equal color distribution for red, blue and brown but with only fourteen ones black and only one yellow.

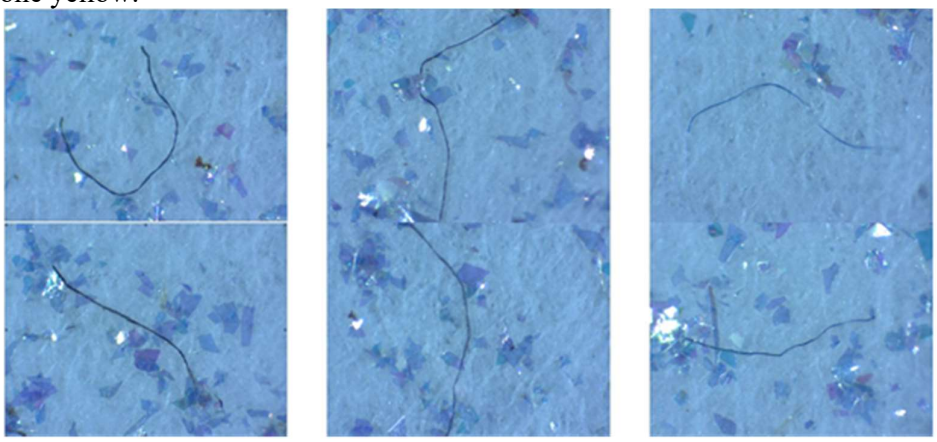

Figure 9. *Optical microscopy for BBS sample (Stemi-2000c 40X)*

The total number of the MPs observed on the filtered sample from the beauty products category and the overall distribution by color of the MPs are presented in Figures 10 and 11.

Figure 10. *Total number of the MPs discovered on filters surface (for the studied beauty products)*

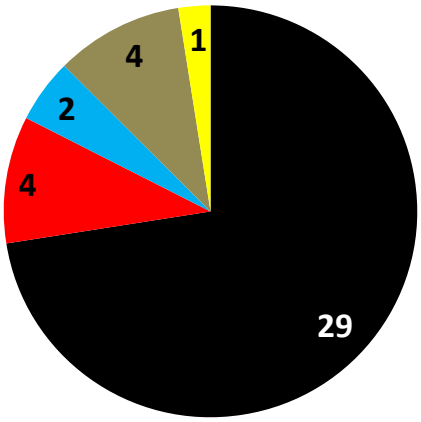

Figure 11. *Overall distribution by color of the MPs identified on filters surface (in the case of beauty products)*

One of the known analytical methods used for both morphological and chemical identification of microplastic particles is μ-FTIR. Briefly, this imagining technique highly used in MPs investigation combines IR spectroscopy with IR microscope. Even that μ-FTIR spectroscopy takes more time to obtain the desired imagines in terms of MPs, this method represents one of the best choices to characterize the specific bonds present in a polymeric molecule type, based on vibrational frequency. In this regard, in this study transmission mode/attenuated total reflection (ATR) mode, depending on MPs sample, was applied. The FTIR spectra obtained for MPs collected from both skin beauty product

and skin care products (i.e., shower gels and body sprays), the overlaps spectra (comparative with blank filter), the possible assignments and MPs images, are presented in Figures 12 - 19 and Tables 4 - 6. At first glance of blank filter (Figure 12 and Table 4) most particles are of natural origin such as cellulose. Particularly, fibrous particles can be seen and are of cellulosic origin.

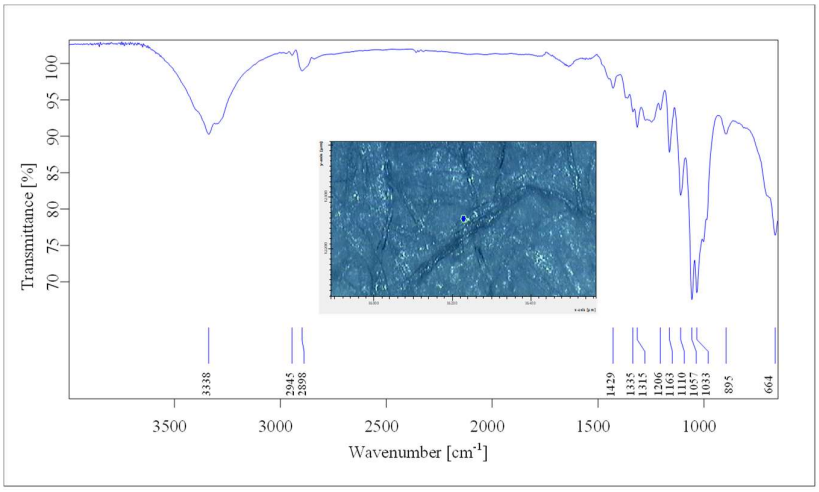

Figure 12. *IR spectrum and μ-FTIR image of cellulosic filter*

Table 4. *Infrared transmittance peaks [cm^{-1}]and relative intensity of cellulosic filter*

Peaks [cm^{-1}]and relative intensity	**Assignments**
664s	NH bending, C=O bending
895w	C–C stretching
1033m	C–C stretching
1057m	aromatic CH bending/C–O stretching
1110m	C–C stretching
1163m	CH bending, CH_3 rocking, C–C stretching
1206w	CH_3 rocking, C–C stretching
1315w	CH_3 bending
1335w	CH_3 bending
1429w	Aromatic ring stretching
2898w	C–H stretching
2945w	C–H stretching
3338w	cellulosic structure
s-strong; m-medium; w-weak	

Figures 13 - 15 show the IR spectra and μ-FTIR images for samples CtGD, NaGD and NiGD. From the above-mentioned figures and Table 5 were identified several functional groups assigned mainly to polypropylene (PP), polyethylene terephthalate (PET), cellulose acetate (CA); the overlaps of IR spectra for CtGD, NaGD and NiGD samples compared with cellulose filter (Figure 16) show several similitudes excepting NiGD sample.

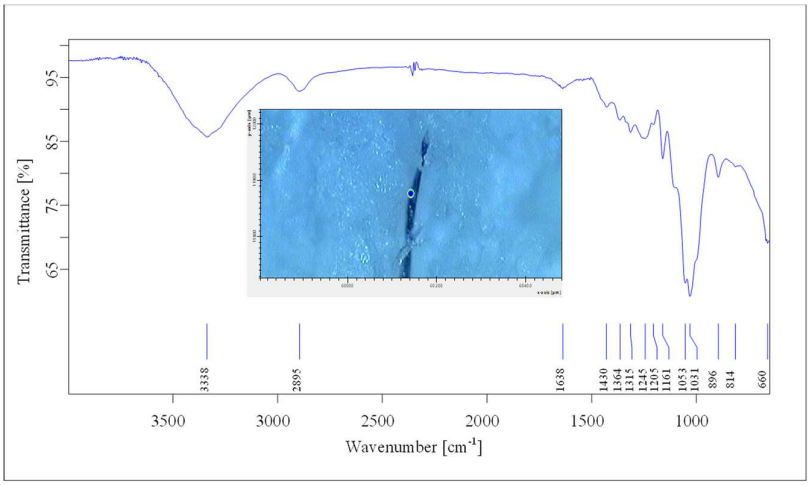

Figure 13. *IR spectrum and μ-FTIR image of MP isolated in CtGD sample*

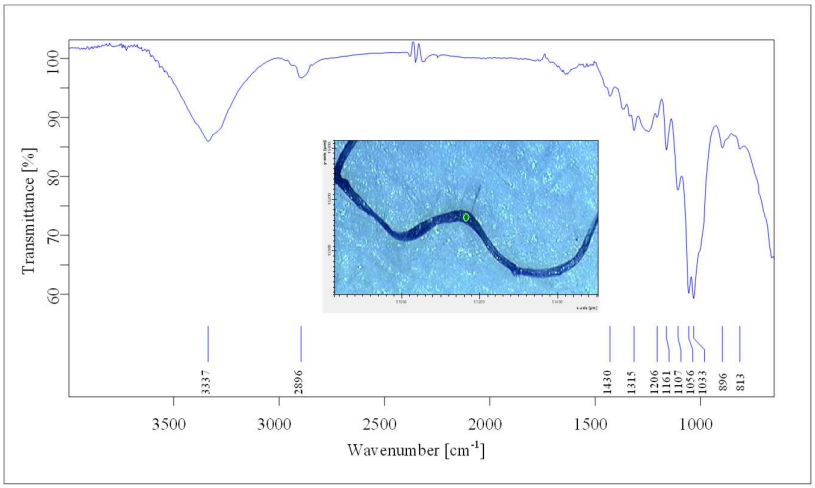

Figure 14. *IR spectrum and μ-FTIR image of MP isolated in NaGD sample*

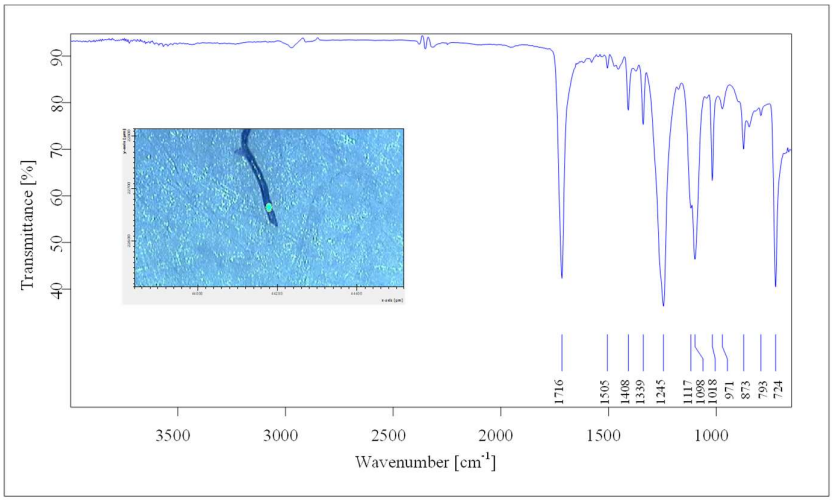

Figure 15. *IR spectrum and μ-FTIR image of MP isolated in NiGD sample*

Table 5. *Comparative IR data for the samples from the personal care products category*

CtGD	NaGD	NiGD	Assignments	Possibly from
-	-	724s	Aromatic CH out of plane bend/CH_2 rocking	High density polyethylene (HDPE) / Low density Polyethylene (LDPE)
-	-	793s	CH_2 rocking, C–C stretching, C–CH stretching	High density polyethylene (HDPE) / Low density Polyethylene (LDPE)
814w	813w	-	CH_2 rocking, C–C stretching, C–CH stretching	Polypropylene (PP)
896w	896w	873m	Aromatic ring stretching or CH bending	Cellulose acetate (CA)
-	-	971w	CH_3 rocking, C–C stretching	Polypropylene (PP)
1031w	1033w	1018s	Aromatic CH bending	Polystyrene (PS)
1053w	1056w	1098s	C–O stretching	Polyethylene terephthalate (PET)
-	1107w	1117w	C–O stretching	Polyvinyl chloride (PVC)
1161m	1161m	-	CH bending, CH_3 rocking, C–C stretching	Polypropylene (PP)
1205w	1206w	-	CF_2 stretching, CH_2 bending	Polytetrafluorethylene (PTFE)
1245w	-	1245s	C–O stretching	Polyethylene terephthalate (PET)
1315w	1315w	-	C–O stretching	Polyethylene terephthalate (PET)
1336w	-	1339m	CH bending	Polyvinyl chloride (PVC)
1430w	1430w	1408m	CH_2 bending	Polymethyl methacrylate (PMMA)
-	-	1505w	Aromatic ring stretching	Polycarbonate (PC)
-	-	1716s	C=O stretching	Polyethylene terephthalate (PET)
2895w	2896w	-	C=O stretching	Polypropylene (PP)
3338w	3337w	-	Cellulosic structure	Cellulose acetate (CA)
s-strong; m-medium; w-weak				

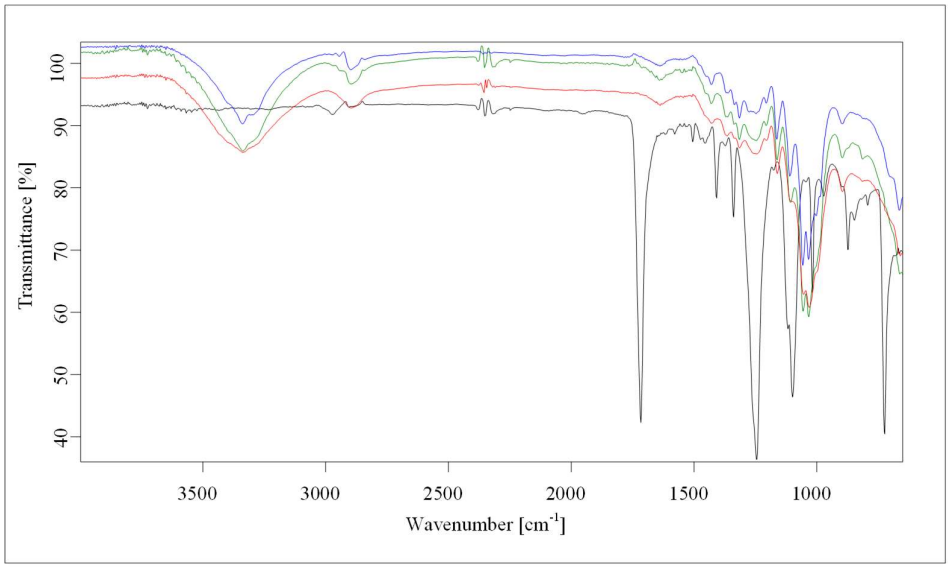

Figure 16. *Overlap of IR spectra for personal care products: blue=cellulosic filter; green= NaGD; red = CtGD; black = NiGD*

Figures 17 and 18 show the IR spectra and μ-FTIR images for samples BBS and IBS. From these figures and Table 6 were identified several functional groups assigned mainly to polypropylene (PP), polyethylene terephthalate (PET), and cellulose acetate (CA); the overlaps of IR spectra for BBS and IBS samples compared with cellulose filter (Figure 19) show similitudes regarding the obtained peaks (same signals).

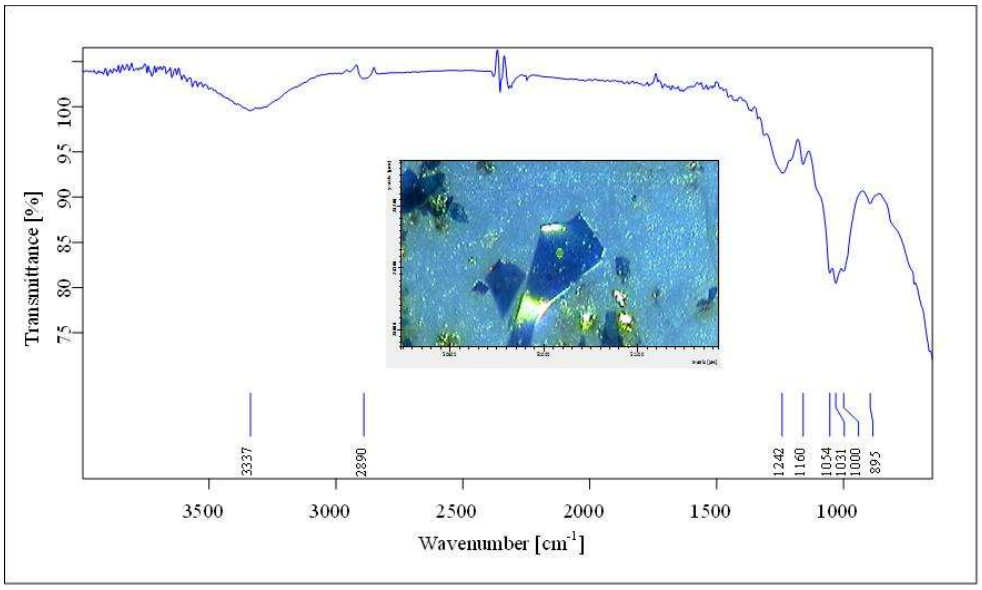

Figure 17. *IR spectrum and μ-FTIR image of MP isolated in IBS sample*

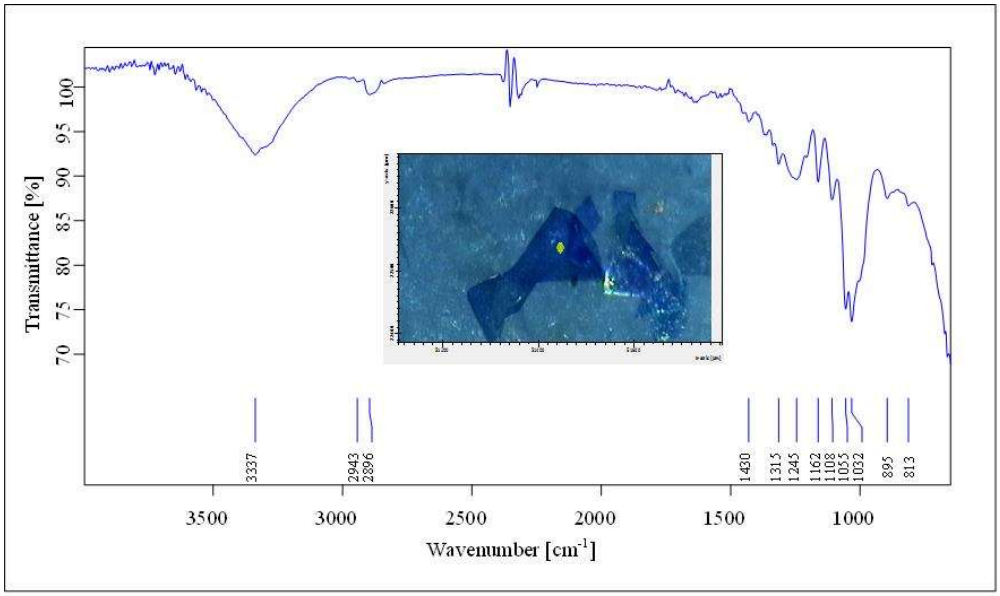

Figure 18. *IR spectrum and μ-FTIR image of MP isolated in BBS sample*

Table 6. *Comparative IR data for samples from the beauty products category*

IBS	BBS	Assignments	Possibly from
-	813w	CH_2 rocking, C–C stretching, C–CH stretching	Polypropylene (PP)
895w	895w	Aromatic ring stretching or CH bending	Cellulose acetate (CA)
1000w	-	C–C stretching	Polypropylene (PP)
1031w	1032w	Aromatic CH bending/C–O stretching	Polystyrene (PS) / Ethylene vinyl acetate (EVA)
1054w	1055w	C–O stretching	Polyethylene terephthalate (PET)
-	1108w	C–C stretching	Polyvinyl chloride (PVC)
1160w	1162m	CH bending, CH_3 rocking, C–C stretching	Polypropylene (PP)
1242w	1245w	CF_2 stretching, CH_2 bending	Polytetrafluorethylene (PTFE)
-	1313w	C–O stretching/C(=O)O stretching	Polyethylene terephthalate (PET) / Ethylene vinyl acetate (EVA)
-	1430w	CH_2 bending	Polymethyl methacrylate (PMMA)
2890w	2896w	C–H stretching	Polypropylene (PP)
-	2943w	C–H stretching	Polypropylene (PP)
3337w	3337w	Cellulosic structure	Cellulose acetate (CA)
s-strong; m-medium; w-weak			

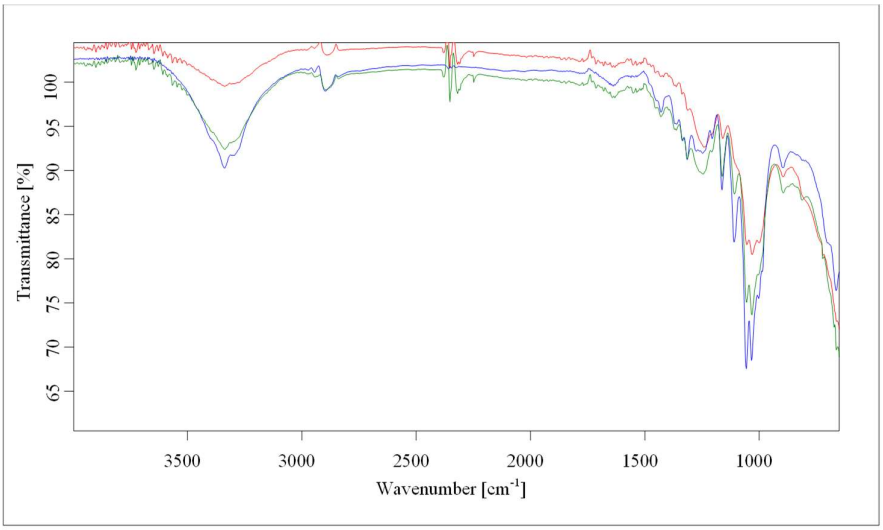

Figure 19. *Overlap of IR spectra for beauty products: blue=cellulosic filter; green=BBS; red = IBS*

The current study could not be completed if the correlation between the analytical results obtained by optical microscopy and µ-FTIR techniques would prove incongruous. MPs identified by optical microscopy were quantified and characterized accordingly to the shape and color but also by means of µ-FTIR analyses was possible the identification of the specific bonds which to confirm the presence of MPs in all studied samples (i.e., shower gel, body spray).

CONCLUSIONS

These studies allowed to investigate the morphology and chemical composition of MPs from two categories of personal care products (i.e., shower gel, body spray) by using optical microscopy (OM) and μ-FTIR. It can be noticed that in this study a series of sample preparation methods as well as related analytical methodologies were developed. This research is a first step to identify and quantify microplastics in organic compound-rich samples such as personal care products. Based on the results of the study it can be concluded that some polymer structures (e.g., polypropylene, polyethylene terephthalate etc.) are present in all analyzed samples. μ-FTIR spectroscopy is a strong and valuable method in microplastic analysis, allowing further study and understanding of microplastics in PCCPs. In addition, μ-FTIR imaging, combined with optical microscopy, proved to be an accurate way to identify and quantify microplastics in cosmetic samples.

Acknowledgement: This work was supported by the Ministry of Research, Innovation and Digitization, (Institutional Development Projects - RDI Excellence Financing Projects), through the project 43PFE/30.12.2021.

REFERENCES

1. Leslie, H.A.: *Review of μplastics in cosmetics*, IMV Institute for Environmental Studies, **2014**, R14/29;
2. Napper, I.E., Bakir, A., Rowland, S.J., Thompson, R.C.: Characterisation, quantity and sorptive properties of microplastics extracted from cosmetics, *Marine Pollution Bulletin*, **2015**, **99**, 178-185;
3. Secchi, M., Castellani, V., Collina, E., Mirabella, N., Sala,S.: Assessing eco-innovations in green chemistry: Life Cycle Assessment (LCA) of a cosmetic product with a bio-based ingredient, *Journal of Cleaner Production*, **2016**, **129**, 269-281;
4. Lei, K., Qiao, F., Liu, Q., Wei Z., Qi H., Cui S., Yue X., Deng Y.: An, Microplastics releasing from personal care and cosmetic products in China, *Marine Pollution Bulletin*, **2017**, **123**, 122-126;
5. Guerranti, C., Martellini, T., Perra, G., Scopetani, C., Cincinelli, A.: Microplastics in cosmetics: Environmental issues and needs for global bans, *Environmental Toxicology and Pharmacology*, **2019**, **68**, 75-79;
6. Lamprini, A., Athanasia, V., Panagoula, P., Evangelia, P., Vilelmine, C.: Worldwide actions against plastic pollution from microbeads and microplastics in cosmetics focusing on European policies. Has the issue been handled effectively?, *Marine Pollution Bulletin*, **2020**, **162**, 111883;
7. Habib, R.Z., Abdoon, M.M.S., Al Meqbaali, R.M., Ghebremedhin, F., Elkashlan, M., Kittaneh, W.F., Cherupurakal, N., Mourad, A.H.I., Thiemann, T., Al Kindi, A.R.: Analysis of μbeads in cosmetic products in the United Arab Emirates, *Environmental Pollution*, **2020**, **258**, 113831;
8. Thaiba, B.M., Sedai, T., Bastakoti, S., Karki, A., Anuradha, K.C., Khadka, G., Acharya, S., Kandel, B., Giri, B., Neupane, B.B.: A review on analytical performance of micro- and nanoplastics analysis methods, *Arabian Journal of Chemistry*, **2023**, **16** (5), 104686;
9. Cheung, P.K., Fok, L.: Characterisation of plastic microbeads in facial scrubs and their estimated emissions in Mainland China, *Water Resources*, **2017**, **122**, 53-61;
10. Loretz, L.J., Api, A.M., Babcock, L., Barraj, L.M., Burdick, J., Cater, K.C., Jarrett, G., Mann, S., Pan, Y.H.L., Re, T.A., Renskers, K.J., Scrafford, C.G.; Exposure data for cosmetic products: facial cleanser, hair conditioner, and eye shadow, *Food and Chemical Toxicology*, **2008**, **46** (5), 1516-1524;
11. Kalcíkova, G., Gotvajn, A.Z., Kladnik, A., Jemec, A.: Impact of polyethylene microbeads on the floating freshwater plant duckweed Lemna minor, *Environmental Pollution*, **2017**, **230**, 1108-1115;

12. Chang, M.: Reducing microplastics from facial exfoliating cleansers in wastewater through treatment versus consumer product decisions, *Marine Pollution Bulletin*, **2015**, **101**(1), 330-333;
13. Fendall, L.S., Sewell, M.A.; Contributing to marine pollution by washing your face: microplastics in facial cleansers, *Marine Pollution Bulletin*, **2009**, **58** (8), 1225-1228;
14. Gregory, M.R.: Plastic 'scrubbers' in hand cleansers: a further (and minor) source for marine pollution identified, *Marine Pollution Bulletin*, **1996**, **32** (12), 867-871;
15. Altunışık, A.: Prevalence of microplastics in commercially sold soft drinks and human risk assessment, *Journal of Environmental Management*, **2023**, **336**, 117720;
16. Bashir, S.M., Kimiko, S., Mak, C.W., Fang, J.K.H., Concalves, D.: Personal Care and Cosmetic Products as a Potential Source of Environmental Contamination by Microplastics in a Densely Populated Asian City, *Frontiers in Marine Science*, **2021**, **8**, 683482;
17. Lithner, D, Larsson, Å., Dave, G.: Environmental and health hazard ranking and assessment of plastic polymers based on chemical composition, *Science of the Total Environment*, **2011**, **409**, 3309-3324;
18. Parashar, N., Hait, S.: Recent advances on microplastics pollution and removal from wastewater systems: A critical review, *Journal of Environmental Management*, **2023**, **340**, 118014;
19. Rocha-Santos, T., Duarte, A.C.: A critical overview of the analytical approaches to the occurrence, the fate and the behavior of microplastics in the environment, *TrAC Trends in Analytical Chemistry*, **2015**, **65**, 47-53;
20. Pelegrini, K., Pereira, T.C.B., Maraschin, T.G., De Souza Teodoro, L., De Souza Basso, N.R., Barrera De Galland, G.L., Ligabue, R.A., Bogo, M.R.: Micro- and nanoplastic toxicity: A review on size, type, source, and test-organism implications, *Science of the Total Environment*, **2023**, **878**, 162954;
21. Zhang, F., Xu, J., Wang, X., Jabeen, K., Li, D.: Microplastic contamination of fish gills and the assessment of both quality assurance and quality control during laboratory analyses, *Marine Pollution Bulletin*, **2021, 173** (B), 113051;
22. Sridhar, A., Kannan, D., Kapoor, A., Prabhakar, S.: Extraction and detection methods of microplastics in food and marine systems: A critical review, *Chemosphere*, **2022**, **286** (1), 131653;
23. Nasse, M.J., Walsh, M., Mattson, E.C., Reininger, R., Kajdacsy-Balla, A., Macias, V., Bhargava, R., Hirschmugl, C.: High-resolution Fourier-transform infrared chemical imaging with multiple synchrotron beams, *Nature Methods*, **2011**, **8** (5), 413-416;
24. Renner, G., Nellessen, A., Schwiers, A., Wenzel, M., Schimidit, T.C., Schram, J.: Data preprocessing & evaluation used in the microplastics identification process: A critical review & practical guide, *TrAC Trends in Analytical Chemistry*, **2019**, **111**, 229-238;
25. Cowger, W., Gray, A., Christiansen, S.H., DeFrond, H., Deshpande, A.D., Hemabessiere, L., Lee, E., Mill, L., Munno, K., Ossmann, B.E., Pittroff, M., Rochman, C., Sarau, G., Tarby, S., Primpke, S.: Critical review of processing and classification techniques for images and spectra in microplastic research, *Applied Spectroscopy*, **2020**, **74** (9), 989-1010;
26. Xu, J.L., Thomas, K.V., Luo, Z., Gowen, A.A.: FTIR and Raman imaging for microplastics analysis: State of the art, challenges and prospects, *TrAC Trends in Analytical Chemistry*, **2019**, **119**, 115629;
27. Chen, Y., Zou, C., Mastalerz, M., Hu, S., Gasaway, C., Tao, X.: Applications of Micro-Fourier Transform Infrared Spectroscopy (FTIR) in the Geological Sciences – A Review, *International Journal of Molecular Sciences*, **2015**, **16** (12), 30223-30250;
28. Finnegan, A., Susserott, R.C., Koh, L.H., Teo, W.B., Gouramanis, C.: A Simple Sample Preparation Method to Significantly Improve Fourier Transform Infrared (FT-IR) Spectra of Microplastics, *Applied Spectroscopy*, **2022**, **76** (7), 783-792;
29. Harrison, J.P., Ojeda, J.J.: Romero-Gonzalez M. E., The applicability of reflectance micro-Fourier-transform infrared spectroscopy for the detection of synthetic microplastics in marine sediments, *Science of The Total Environment*, **2012**, **416**, 455-463;
30. Bec, K.B., Huck, C.W.: Advances in Near-Infrared Spectroscopy and Related Computational Methods, *Molecules*, **2019**, **24** (23), 4370;
31. Elliott, A.D.: Confocal Microscopy: Principles and Modern Practices, *Current Protocols in Cytometry*, **2020**, **92** (1), e68;
32. Brown, C.M.: Fluorescence microscopy - avoiding the pitfalls, *Journal Cell Science*, **2007**, **120** (10), 1703-1705;

33. Chua, L., Banas, A., Banas, K.: Comparison of ATR–FTIR and O-PTIR Imaging Techniques for the Characterisation of Zinc-Type Degradation Products in a Paint Cross-Section, *Molecules*, **2022**, **27** (19), 6301;
34. Joseph, E., Ricci, C., Kazarian, S.G., Mazzeo, R., Prati, S., Ioele, M.: Macro-ATR-FT-IR spectroscopic imaging analysis of paint cross-sections, *Vibrational Spectroscopy*, **2010**, **53** (2), 274-278;
35. Wrobel, T.P., Marzec, K.M., Majzner, K., Kochan, K., Bartus, M., Chlopicki, S., Baranska, M.: Attenuated total reflection Fourier transform infrared (ATR-FTIR) spectroscopy of a single endothelial cell, *Analyst*, **2012**, **137** (18), 4135-4139;
36. Meyvisch, P., Gurdebeke, P.R., Louwye, S., Versteegh, G., Mertens, K.N., Vrielinck, H.: Attenuated Total Reflection (ATR) Micro-Fourier Transform Infrared (Micro-FT-IR) Spectroscopy to Enhance Repeatability and Reproducibility of Spectra Derived from Single Specimen Organic-Walled Dinoflagellate Cysts, *Applied Spectroscopy*, **2022**, **76** (2), 235-254;
37. Olteanu, R.L., Radulescu, C., Stihi, C., Dulama, I.D., Nicolescu, C.M., Bucurica, I.A., Gurgu, I.V., Stirbescu, R.M., Gheboianu, A.I., Let, D.D., Teodorescu, S., Olteanu, L., Stirbescu, N.M.: Indoor microclimatic variables assessment by vibrational spectroscopy on original structure of Tropaeum Traiani monument, Adamclisi, *Journal of Science Arts*, **2020**, **20** (4), 977-994;
38. https://citius.us.es/web/serv_documento_equipo.php?file=3f95632c4, HYPERION Series FT-IR Microscopes Brochure, accessed May 24th, 2023.